Adaptive Hysteresis-Band Current Controller of a Three Phase Induction Machine

Dr. Rami A. Mahir
(Professor)
University of Technology
Control and Sysetm Engineering . Dep.

Dr. Amjad J.H.
(Lecturer)
University of Technology
Control and Sysetm Engineering . Dep.

Mr. Ayad Q. Hussien
(Assist Lecturer)
Foundation of Technical Education
(ElectricalTehhnical College)

Abstract:

Hysteresis current control is one of the simplest techniques used to control the magnitude and phase angle of three phase motor currents for high-speed drive systems. It is well-known of its simplicity of implementation and inherent peak current limiting capability. However, conventional fixed-band hysteresis control has a variable switching frequency throughout the fundamental period, and consequently the load current harmonic ripple is not optimal.

In this paper, an adaptive hysteresis band current controller (HBCC) is described and its performance and effectiveness is checked in case of the presence and absence of the speed loop of indirect field-oriented controlled induction machine (IFOC IM).

الخلاصـــــــة:

إن السيطرة على تيارات المحركات الحثية باستخدام تقنية عرض الهسترة هو من ابسط التقنيات المستخدمة للسيطرة على زاوية وقيمة التيارات لمسوقات القدرة ذوات الأداء العالي. وتتميز هذه التقنية بسهولة تنفيذها وقابليتها على تحديد قيمة التيار. ومع ذلك فان من أهم مساوئ هذه الطريقة هو تغير تردد الغلق وبالتالي فان التمور التوافقي لتيار الحمل لا يكون مثاليا".

يقـدم هذا البحث وصفا" تفصيليا" لتقنية توليف مسيطر تيار ذو عرض هسترة متغير لغرض تحقيق تردد غلق ثابت. تم دراسة اداء هذا المسيطر ذو عرض الهسترة المتغير(HBCC) في حالة وجود وعدم وجود دارة السرعة (Speed loop) لماكنة مسيطر على مجالها باستخدام طريقة توجيه المجال الغير مباشر (IFOC)، حيث أن المنحنيات الناتجة من المحاكات تثبت غاية هذا البحث.

1. Introduction:

Hysteresis current control is a method of controlling a voltage source inverter so that an attempt current is generated which follows a reference current waveform. This method controls the switching in an inverter asynchronously to ramp the current through an inductor up and down so that it follows a reference. Hysteresis current control is the easiest control method to implement. This method also exhibits robustness feature [1,2].

A low-cost current regulator using hysteresis is shown in Fig.(1). In this controller the desired current of a given phase, say i_a^*, is summed with the negative of the measured, i_a.

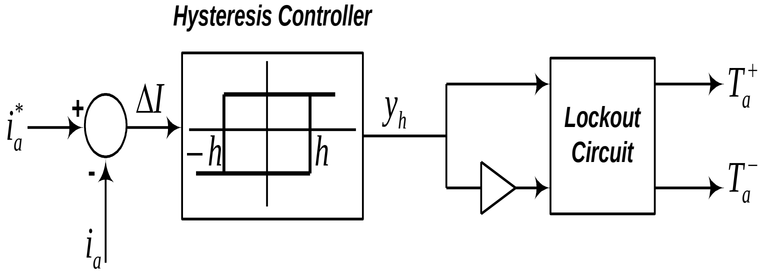

Figure (1) Hysteresis current controller

The error is fed to a comparator having a prescribed hysteresis band $2\Delta I$. The hysteresis output y_h that governs the leg switching of the converter can be described as : [3]

$$if \;\; \Delta I > h \;\; Then \;\; y_h = 1,$$

$$if -h \le \Delta I \le h \; and \; d\Delta I/dt > 0 \;\; Then \;\; y_h = 1,$$

$$if -h \le \Delta I \le h \; and \; d\Delta I/dt < 0 \;\; Then \;\; y_h = -1$$

$$if \;\; \Delta I < -h \;\; Then \;\; y_h = -1.$$

Switching of the leg of the inverter (T_A^+ off, T_A^- on) occurs when the current attempts to exceed a value set corresponding to the desired current ($i_a + \Delta I$). The reverse switching (T_A^+ on, T_A^- off) occurs when the current attempts to become less than ($i_a - \Delta I$). A "lockout circuit" is normally incorporated to allow for inverter switch recovery time and thus avoid short circuits across the dc link.

Unfortunately, with this type of control the switching frequency does not remain constant but varies along different portions of the desired current waveform due to the effect of the emf.

Fig.(2) shows a typical waveform illustrating the variable nature of the PWM switching frequency.Unfotunat- ely, the variation of the switching rate is also opposite to the needs for good current control with the highest switching rates associated with the lowest reference frequencies. The hysteresis controller also has the somewhat unexpected property of limiting the current error to twice the hysteresis band rather than to a value within the band itself.

The switching frequency can be altered by the width of the hysteresis band, the size of the inductor that the current flows through and the DC voltage applied to the inductor by the inverter [1]. Fixed modulation frequency has been achieved by a variable width of the hysteresis band as function of the instantaneous output voltage [4,5].

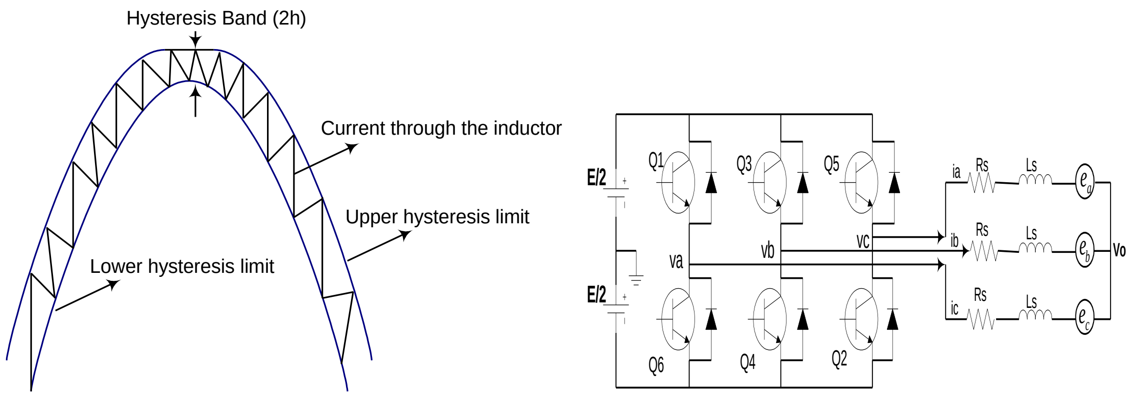

Figure (2) Hysteresis current waveforms for one phase

2. Principle of Adaptive Control Approach for Hysteresis Current Controller:

The basic structure of a current-controlled variable speed drive is shown in Fig.(3), and consists of a three phase Voltage Source Inverter (VSI) driving a three phase motor, which is represented as a three phase set of back emf's behind series resistance and reactance [4,5].

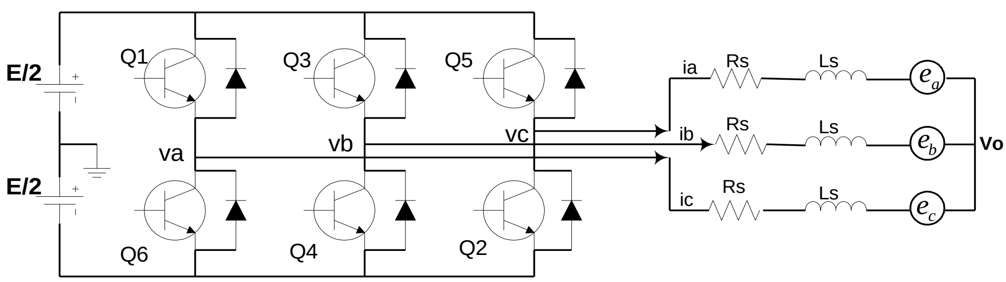

Fig.(3) Three-Phase inverter with isolated neutral motor

Hysteresis current control for this system involves the measurement of the current flowing in each phase leg of the motor, the comparison of this current with a given reference current, and the switching of each phase leg of the inverter to the upper or the lower dc supply rails as appropriate to keep the measured current within an error band compared to the reference current [5,6].

If one considers the three-phase inverter with isolated neutral motor load shown in Fig.(3), the machine back emf voltages can mutually interact. Since the VSI and the AC motor are symmetrical, one phase only needs to be considered so that for phase **a**, the phase voltage and current relationship becomes:

$$v_a = L_s \frac{di_a}{dt} + r_s i_a + e_a + v_o \tag{1}$$

where v_o is the motor neutral voltage referred to the supply midpoint. Similar expressions can be written for phases b and c.

In practice, v_a can only take the values of $\pm V_{dc}$, depending on the state of the phase leg switches. However, if the ideal reference current i_a^* is assumed to flow through phase **a** of the motor, then a fictitious phase voltage v_a^* would exist, given by:

$$v_a^* = L_s \frac{di_a^*}{dt} + r_s i_a^* + e_a \tag{2}$$

In this case, both v_a^* and i_a^* are sinusoidal functions and $i_o^*=0$. Since the motor neutral point is isolated, the instantaneous sum of three currents $i_{as}+i_{bs}+i_{cs}=0$. Hence, summing the three phase voltage equations gives:

$$v_o = (v_a + v_b + v_c)/3 \tag{3}$$

Equation (3) shows that even if the neutral point voltage is not directly available, v_o can still be determined from the inverter phase voltages [6].

For hysteresis-band current control, the difference between the actual and the reference current can be defined as ε_a, where:

$$\varepsilon_a = i_a^* - i_a \tag{4}$$

So, subtracting (1) from (2) gives:

$$v_a^* - v_a = L_s \frac{d(i_a^* - i_a)}{dt} + r_s.(i_a^* - i_a) - v_o \tag{5}$$

which can be described as a first order linear differential equation with two forcing functions of $v_a^* - v_a$ and v_o. From Eq.(4), the current response function $(i_a^* - i_a)$ can also be decoupled into two parts, viz.:

$$\varepsilon_a = \left(i_a^* - i_a\right) = \zeta_a + \gamma_a \tag{6}$$

where ζ_a =non interacting error w.r.t. v_o.

and γ_a =interacting error w.r.t. v_o.

Hence Eq.(4) can be separated into sections as follows

$$v_a^* - v_a = L_s \frac{d\zeta_a}{dt} + r_s \zeta_a \tag{7}$$

$$v_o = L_s \frac{d\gamma_a}{dt} + r_s \gamma_a \tag{8}$$

For a reasonably high switching frequency, the effect of the resistance r_s can be neglected, so that (7) becomes [6].

$$v_a^* - v_a = L_s \frac{d\zeta_a}{dt} \tag{9}$$

The operation of the hysteresis current controller over one switching cycle is shown in Fig.(4), with straight lines substituted for the sinusoidal current reference and error band limits because of the short period of time considered. As can be seen, the phase leg switches of $+V_{dc}/2$ when the motor current i_a becomes less than $h/2$ below the reference, which causes the motor current to begin to increase again.

When i_a reaches the upper error boundary (greater than $h/2$ above the reference), the phase leg switches to $-V_{dc}/2$, and the motor current begins to reduce again [6,7].

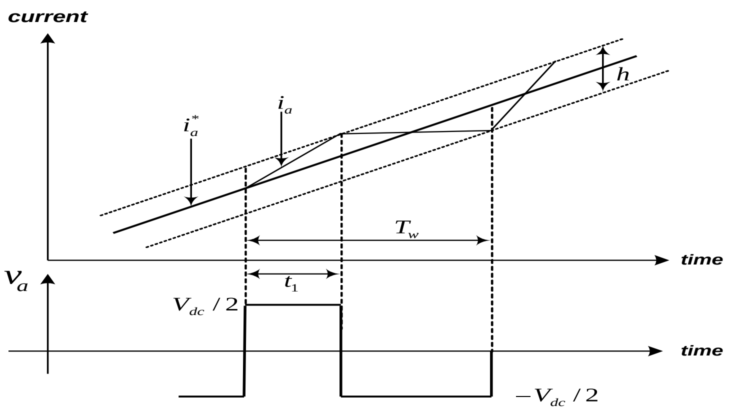

Figure (4) Hysteresis-band current and phase leg voltage waveforms.

From (9), this can be expressed mathematically as:

$$v_a^* - \frac{V_{dc}}{2} = L_s . \frac{\Delta\zeta_a}{\Delta t}$$

$$= L_s . \left\{ \frac{\zeta_a(t_1) - \zeta_a(0)}{t_1 - 0} \right\}$$

$$= L_s \left\{ \frac{-h/2 - h/2}{t_1 - 0} \right\} \qquad 0<t<t_1 \qquad (10)$$

,and

$$v_a^* + \frac{V_{dc}}{2} = L_s . \frac{\Delta\zeta_a}{\Delta t}$$

$$= L_s . \left\{ \frac{\zeta_a(T) - \zeta_a(0)}{T - t_1} \right\}$$

$$= L_s \left\{ \frac{h/2 + h/2}{T_w - t_1} \right\} \qquad \mathbf{0<t<} T_w \qquad \mathbf{(11)}$$

For the period From (10) and (11) the overall time period for one complete switching transition can be shown to be:

$$T_w = \frac{L_s.h.V_{dc}}{(V_{dc}/2)^2 - (v_a^*)^2} \qquad \textbf{(12)}$$

Where T_w is the reciprocal of the switching frequency f_w.

Substituting (9) into (12) and simplifying gives:

$$T_w = \frac{\alpha}{1-(\beta.v_a + \delta.\frac{d\zeta_a}{dt})^2}.h \qquad \textbf{(13)}$$

where:

$\alpha = 4\,L_s/V_{dc}$

$\beta = 2/V_{dc}$

$\delta = 2\,L_s/V_{dc}$

h = hysteresis error band (initially fixed at $h_{\max}$)

From (13), it can be seen that if the error band h (for phase a) is made to vary as:

$$h_a = h_{\max}(1-(h.v_a + \delta.\frac{d\zeta_a}{dt})^2) \qquad \textbf{(14)}$$

The switching frequency f_w will become constant. Phase b and c must be similarly treated to develop hysteresis band expressions for h_b and h_c.

In Laplace form, (14) becomes:

$$h_a(s) = h_{\max}.(1-(\beta.U_a(s) + \delta.s.\zeta(s))^2) \qquad (15)$$

To determine ζ_a (from 6), it is necessary to determine γ_a, which depends only on u_o, from (6). Substituting (3) into (8) gives:

$$(u_a + u_b + u_c)/3 = L_s \frac{d\gamma_a}{dt} + r_s\gamma_a \tag{16}$$

In laplace transform form, Eq.(16) becomes:

$$\gamma_a(s) = \frac{1/3}{L_s s}\,(U_a(s) + U_b(s) + U_c(s)) \tag{17}$$

where r_s has once again been ignored because of the high switching frequency proposed. Note also that $\gamma_a = \gamma_b = \gamma_c$.

Equations (15) and (17) provide the main strategy for the variable band hysteresis current control since they allow a variable hysteresis band to be defined from each phase independent of the floating neutral voltage, so that each phase leg of the inverter can be made to switch at constant frequency.

Figure (5) shows a s-plane block diagram of one phase of the variable-hysteresis-band current controller, while Fig.(6) shows the overall block diagram of the three phase adaptive current controller resulting from combining Fig.s (1), (2) and (3).

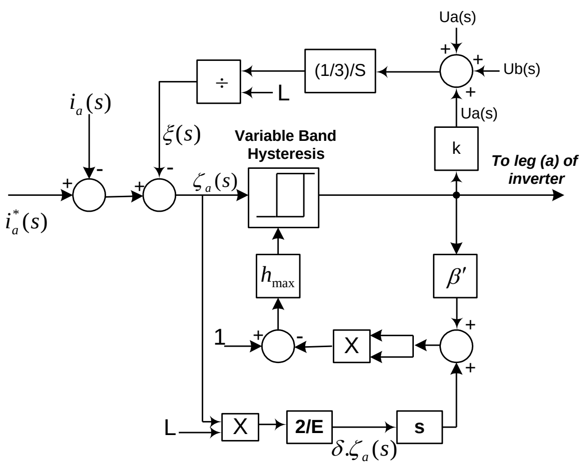

Figure (5) Block diagram for a phase of the adaptive HBCC

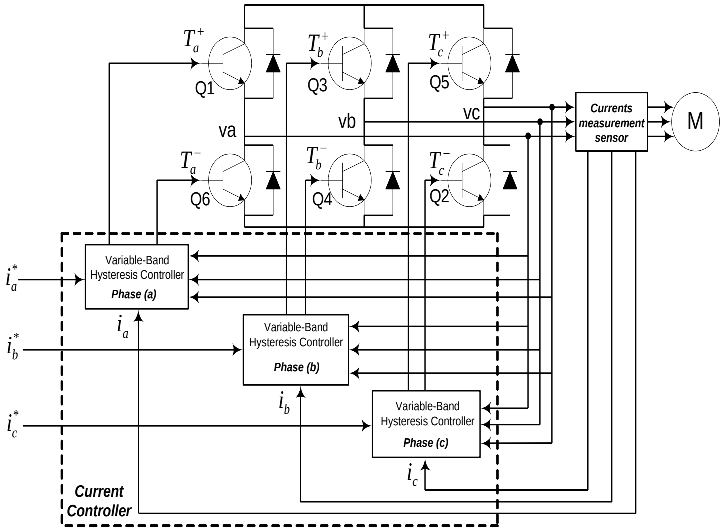

Figure (6) Interconnection of the three adaptive with induction motor and converter

3. Indirect Field Orientation Control (IFOC)

A block diagram of an indirect field orientation controlled (IFOC) induction machine is shown in Fig.(7). It consists of two feedback control loops. The inner loop is a conventional synchronous current regulation loop. The torque command current, i_{qs}^*, is produced by selected controller in the outer speed loop, based on the command speed (ω_r^*) and the actual speed (ω_r) [**3**,**5**,**6**,**7**].

The success of FOC is based on the proper division of stator current into two components; the torque-component i_{qs}^* and magnetizing flux component i_{ds}^*. The indirect FOC method uses a slip equation for partitioning the stator current, as shown in Fig.(7) [**3**,**5**,**8**],

$$\omega_2^* = \frac{r_r'}{L_r'} \frac{i_{qs}^{e*}}{i_{ds}^{e*}} \tag{18}$$

where r_r' and L_r' are the rotor resistance and inductance referred to stationary side respectively. The slip frequency ω_{sl}^* is the difference between the synchronous speed ω_e and rotor speed ω_r. The field orientation angle, θ_e, is the sum of the rotor angle from the position sensor, θ_r, and the angle, θ_{sl}, from the slip speed ω_{sl}. The stator command currents in synchronous frame can be transformed to qd stationary frame using,

$$
\begin{aligned}
i_{qs}^{s*} &= i_{qs}^{e} \cos\theta_e + i_{ds}^{e} \sin\theta_e \\
i_{ds}^{s*} &= -i_{qs}^{e} \sin\theta_e + i_{ds}^{e} \cos\theta_e
\end{aligned}
\tag{19}
$$

Another transformation from *qd* stationary frame to *abc* stator currents is used as follows:

$$
\begin{aligned}
i_{as}^{*} &= i_{qs}^{s*} \\
i_{bs}^{*} &= -(1/2)i_{qs}^{s*} - (\sqrt{3}/2)i_{ds}^{s*} \\
i_{bs}^{*} &= -(1/2)i_{qs}^{s*} + (\sqrt{3}/2)i_{ds}^{s*}
\end{aligned}
\tag{20}
$$

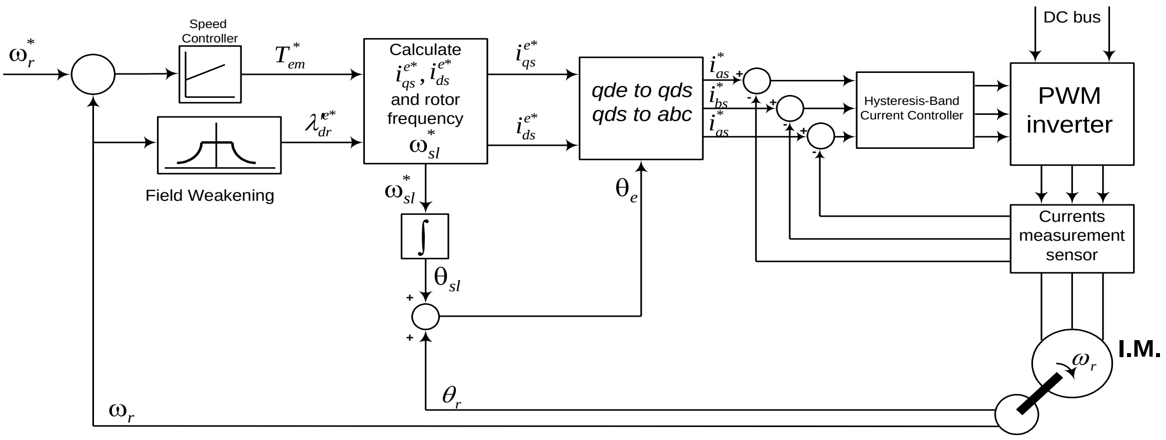

Figure (7) Indirect field-oriented control of a current regulated pwm inverter induction motor drive

However, when a parameter changes, due to saturation and/or heating, the slip calculator will produce incorrect slip commands and the stator current will not be properly partitioned (detuning effect) [3,5,8].

It is worthy to note that the adaptive HBCC is replaced by the conventional HBCC in Fig.(7).The connection of the adaptive HBCC with IFOC IM is shown in Fig.(6), where the circuit diagram of the inverter is replaced with PWM inverter block in Fig.(7). In this paper, the effectiveness of the adaptive HBCC inside the inner loop of IFOC IM is checked in terms of step response, tracking variable speed, disturbance application and the presence of detuning effect.

4. Steady-State Performance of Adaptive Current Controller

The time varying and harmonic charact- eristics of the variable-band hysteresis current control strategy have been studied by simulation.

Figure (8) shows that the SIMULINK is used to model the control strategy equations previously discussed (Fig.5). The control hysteresis equation is written in s-function where a mixing of an m-file with the SIMULINK blocks is performed.

The SIMULINK modeling of the inverter is shown in Fig.(9) [11,12,13]. Therefore, the open loop test of Fig.(6) can by now be achieved by feeding three phase reference currents.

The simulation studies considered the operation of 20 hp IM having the parameters and dynamic model as mentioned in the APPENDIX. The following assumptions were made for simulation purposes:

- The motor was not saturated.
- Back EMFs were sinusoidal.
- The target current references were sinusoidal.

The maximum hysteresis bandwidth was set to achieve a maximum switching frequency of 4kHz for this motor.Figures (10) and (11) compare the suggested adaptive approach against conventional hysteresis control for steady state operation.

The modulation of the hysteresis of the hysteresis error band, and the consequential constant frequency switching and improvement in current control achieved by the new technique can be clearly seen.

Furthermore, comparing the spectral performance of the suggested strategy against the conventional technique, Fig.(12), the reduction in low order harmonics obtained with the variable hysteresis controller is self evident.

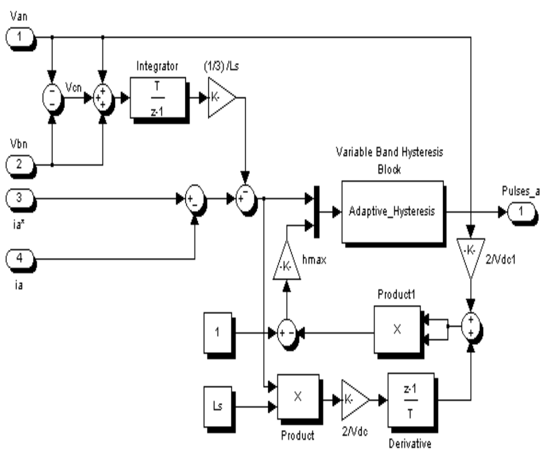

Figure (8) Modeling of adaptive control strategy

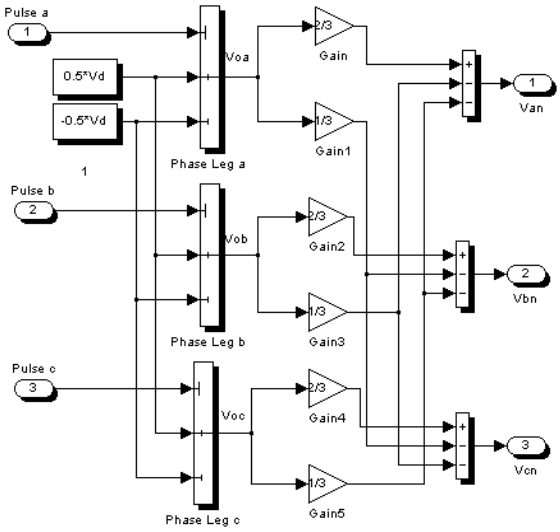

Figure (9) SIMULINK modeling of inverter

5. Dynamic Performance of Adaptive HBCC

In the previous results, the peformance of the adaptive current controller is checked away from the presence of the outer loop; i.e., an open loop is used for that test. By now, the outer loop is involved and the four tests applied to the closed loop drive are again repeated.The details of SIMULINK modeling of adaptive HBCC is shown in Appendix C, Fig.(C). It should be noted that the modulated equation of adaptive hysteresis (Inside Adaptive_Hysteresis Block), eq.(c1), is performed by in s-function file "sfunc_Hysteresis controller" which is listed in Appendix D. Two measurements are required from the closed loop with adaptive HBCC; the FFT plot of the stator current signal and the switching frequency measurement. Therefore, the script file "SA.m" in Appendix D is again used to collect the sampleddata, N=256, during one cycle of the stator current, which are loaded in the MATLAB workspace, and then to compute the FFT of the stator current. In Fig.(13), the IFOC drive is subjected to a step command input. The switching frequency is measured during the two periods of the fundamental current cycle. It can be easily seen from the figure that the stepped command change has not affected the performance of the current controller to eliminate the low order harmonics, nor the switching frequency has been affected significantly; except at the time of a sudden change. The switching frequency is still near the target switching frequency (4kHz), as required. Then, the drive is subjected to cyclic speed reference, of the same characteristics as that described before. Again, the current controller keeps its performance against low order harmo- nics, yet these spectra emerge slightly in the low speed range. But these can be neglected with those spectra near the target switching frequency as seen in Fig.(14). Moreover, the figure shows high switching frequency at the start of command signal and then oscillates near the target frequency.

The detuning effect is tested via doubling the value of the rotor resistor. A degradation in the performance of the current controller in suppressing the low order harmonic is evident in Fig.(15). Again, these spectra are not in the magnitude of those in the neighborhood of the target frequency. The switching frequency is a little far from the target frequency due to this effect. Finally, a sudden disturbance of 10 N.m is applied at 1 second later of drive startup. As seen from Fig.(16), the FFT is not affected by this test and the suppression of low harmonics is evident from the figure. While the switching frequency suffers from a slight change at the time of imposing the disturbance, then it settles to the required one with a slight oscillation near the prescribed frequency.

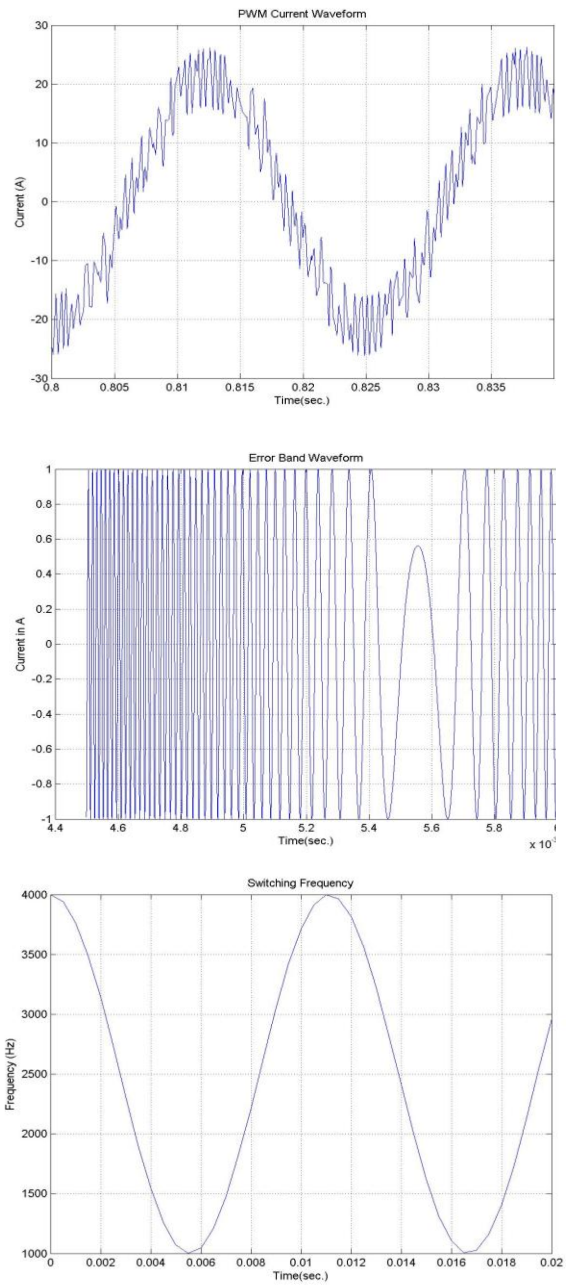

Figure(10)Simulation of conventional HBCC

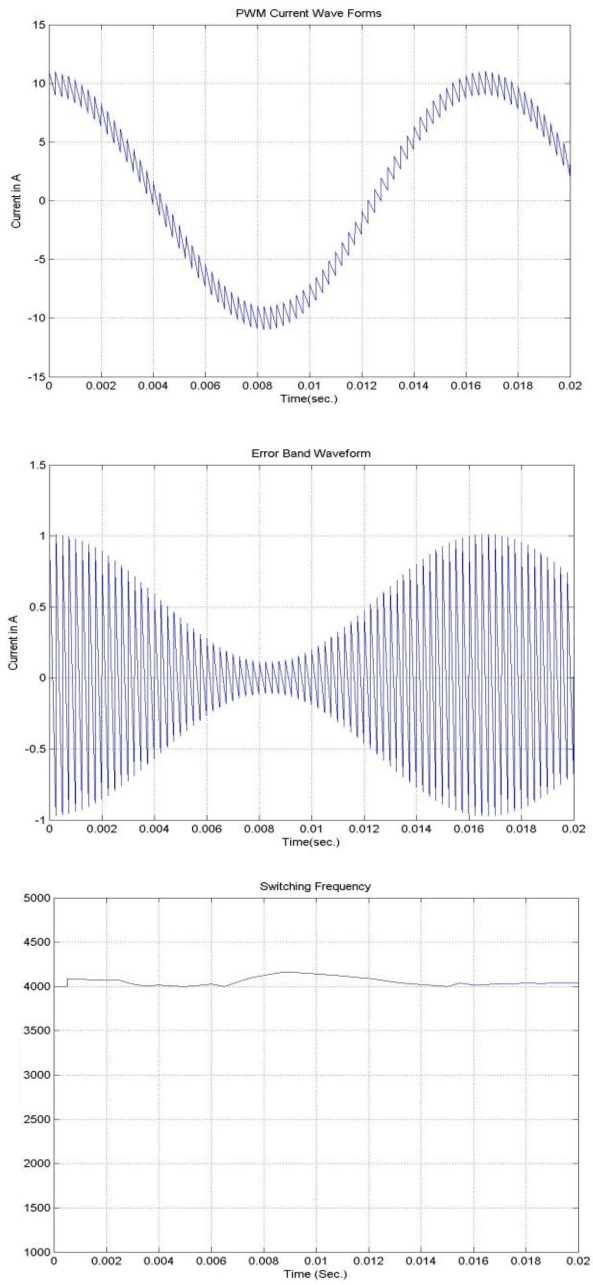

Figure(11)Simulation of adaptve HBCC

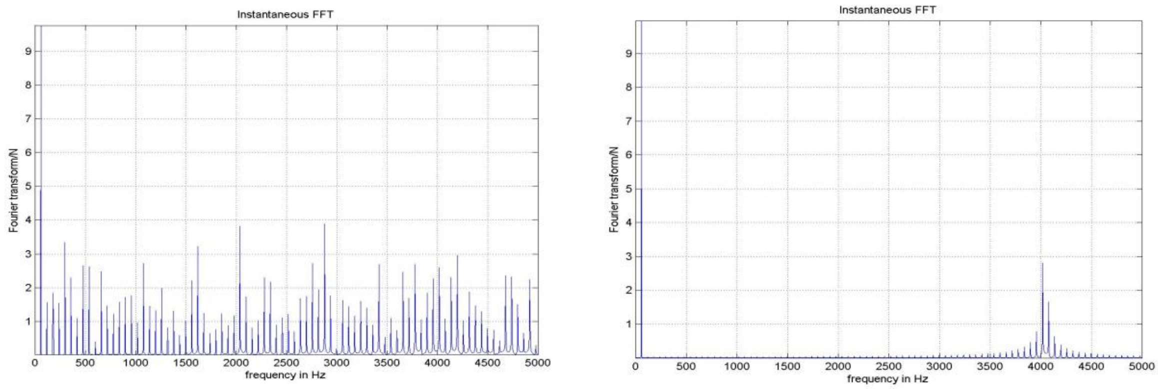

Figure (12) Current Harmonic Spectrums of Conventional and Adaptive HBCC

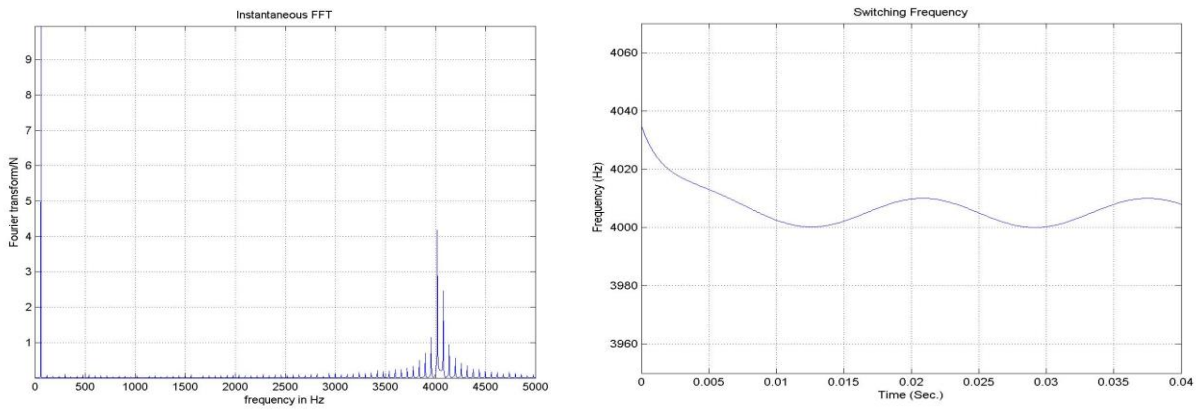

Figure (13) The spectrum of stator current and switching frequency for a step response of I.F.O.C. ac drive with adaptive HBCC.

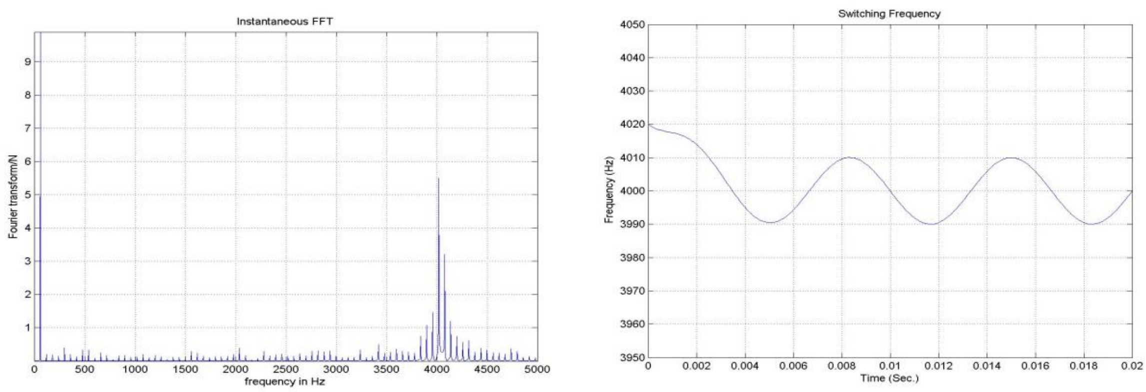

Figure (14) The spectrum of stator current and switching frequency for a tracking response of I.F.O.C. ac drive with adaptive HBCC

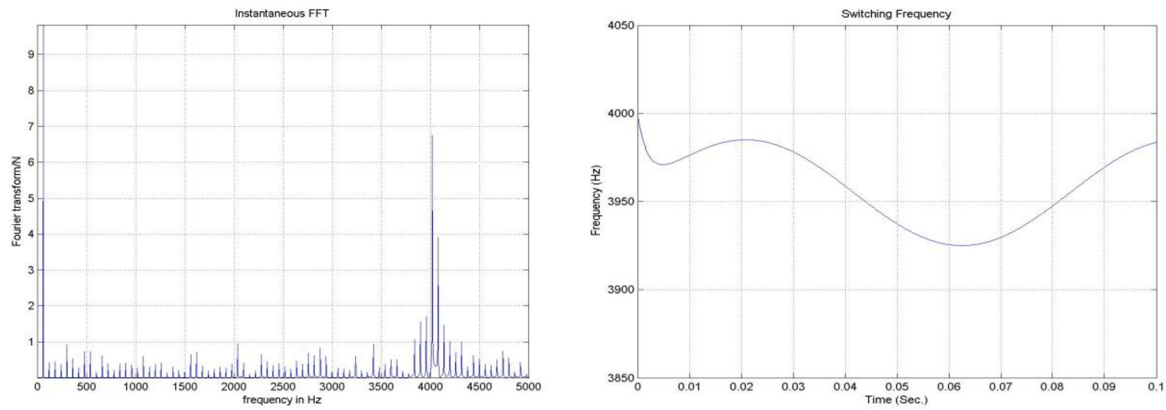

Figure (15) The spectrum of stator current and switching frequency due to the detuning effect.

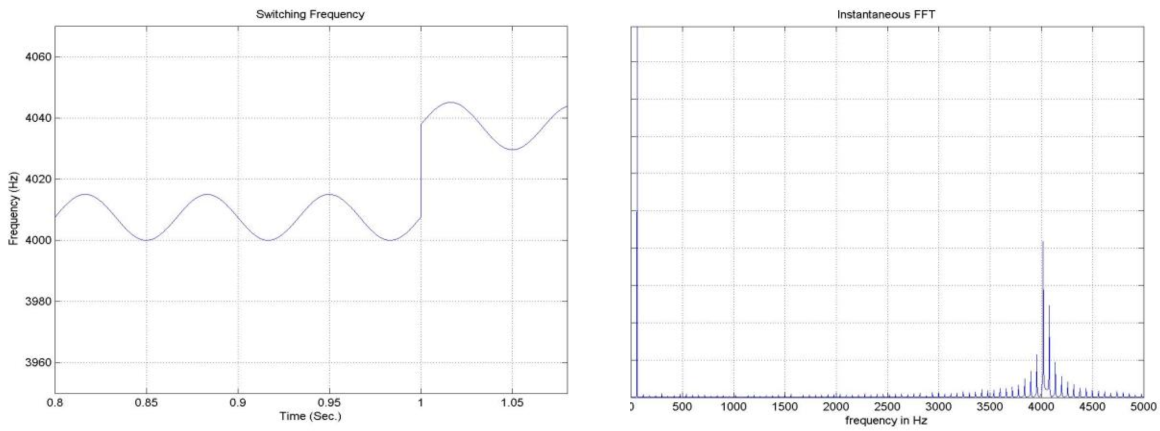

Figure (16) The spectrum of stator current and switching frequency for a sudden change of the applied load

4. Conclusion:

A variable hysteresis band current controller has been described which achieves constant switching frequency without requiring a precise knowledge of the motor parameters. The controller works by using feedback and feedback variables to create a variable hysteresis band envelope, and then compensate for the interaction between phase back-emf's that occurs when the neutral of a three phase is left floating. The results highlighted the following conclusion points:

- Constant frequency switching and improvement in current control achieved by the new technique can be clearly seen.
- The reduction in low order harmonics obtained with the variable hysteresis controller is self-evident.
- The two above privileges achieved by this technique is checked for both open and closed loop (IFOC) tests. The method showed equally improvement in both tests, which will certainly enhance the IFOC drive performance.

APPENDIX

(A)

The parameters of the 20 hp IM are described in Table(1).

Table 1: Induction Motor Parameter

Rated Power	*20 hp*
Rated Line-Line Voltage	*200 V*
Rate Torque	*81.5 Nm*
Number of Poles (P)	*4*
Stator Resistans (rs)	*0.106 Ω*
Stator Inductance (L_s)	*9.15 mH*
Magnetizing Inductance(L_m)	*8.67 mH*
Rotor Resistance(r_s)	*0.076 Ω*
Rotor Inductance (L_s)	*9.15 mH*

(B)

The state-space model for induction motor developed in stationary reference frame, used in the previous study, is given below [3,39,40].

$$\frac{\mathrm{d}}{\mathrm{dt}}\begin{bmatrix} i_{ds}^{s} \\ i_{qs}^{s} \\ \lambda_{dr}^{s} \\ \lambda_{qr}^{s} \\ \omega_r \end{bmatrix} = \begin{bmatrix} -\dfrac{K_R}{K_L} & 0 & \dfrac{L_m r_r'}{L_r'^2 K_L} & \dfrac{L_m \omega_r}{L_r' K_L} & 0 \\ 0 & -\dfrac{K_R}{K_L} & -\dfrac{L_m \omega_r}{L_r' K_L} & \dfrac{L_m r_r'}{L_r'^2 K_L} & 0 \\ \dfrac{L_m}{T_r} & 0 & -\dfrac{1}{T_r} & -\omega_r & 0 \\ 0 & \dfrac{L_m}{T_r} & \omega_r & -\dfrac{1}{T_r} & 0 \\ 0 & 0 & 0 & 0 & 0 \end{bmatrix} \begin{bmatrix} i_{ds}^{s} \\ i_{qs}^{s} \\ \lambda_{dr}^{s} \\ \lambda_{qr}^{s} \\ \omega_r \end{bmatrix} + \frac{1}{K_L}\begin{bmatrix} 1 & 0 \\ 0 & 1 \\ 0 & 0 \\ 0 & 0 \\ 0 & 0 \end{bmatrix}\begin{bmatrix} V_{ds}^{s} \\ V_{qs}^{s} \end{bmatrix}$$

$$\begin{bmatrix} i_{ds}^{s} \\ i_{qs}^{s} \end{bmatrix} = \begin{bmatrix} 1 & 0 & 0 & 0 & 0 \\ 0 & 1 & 0 & 0 & 0 \end{bmatrix} \begin{bmatrix} i_{ds}^{s} \\ i_{qs}^{s} \\ \lambda_{dr}^{\prime s} \\ \lambda_{qr}^{\prime s} \\ \omega_r \end{bmatrix} + \begin{bmatrix} 0 & 0 \\ 0 & 0 \end{bmatrix}\begin{bmatrix} V_{ds}^{s} \\ V_{qs}^{s} \end{bmatrix}$$

where $K_L = (L_r' L_s - L_m^2)/L_r'$ and $K_R = r_s + r_r'(L_m/L_r')^2$. The parameters L_r', L_s, L_m are rotor, stator and main inductances, and $T_r = L_r' / r_r'$ is the rotor time constant.

(C)

Modeling of Adaptive Hysteresis-Band Current Controller

The main equation governing the online adaptation process can be re-written as:

$$\varepsilon_a = \left(i_a^* - i_a\right) = \zeta_a + \gamma_a \qquad \text{(C.1)}$$

$$h_a = h_{\max}(\mathbf{1} - (\beta.U_a + \delta.s.\zeta)^{\mathbf{2}}) \qquad \text{(C.2)}$$

$$\gamma_a(s) = \frac{1/3}{L_s s}(v_a + v_b + v_c) \qquad \text{(C.3)}$$

Equations (C.1)(C.2) and (C.3) provide the strategy for the variable band hysteresis currrent contol since they allow a variable hysteresis band to be defined from each phase so that each phase leg of the inverter can made to switch at constant frequency.

The block digram representing overall current controller is given in fig.(C.1)

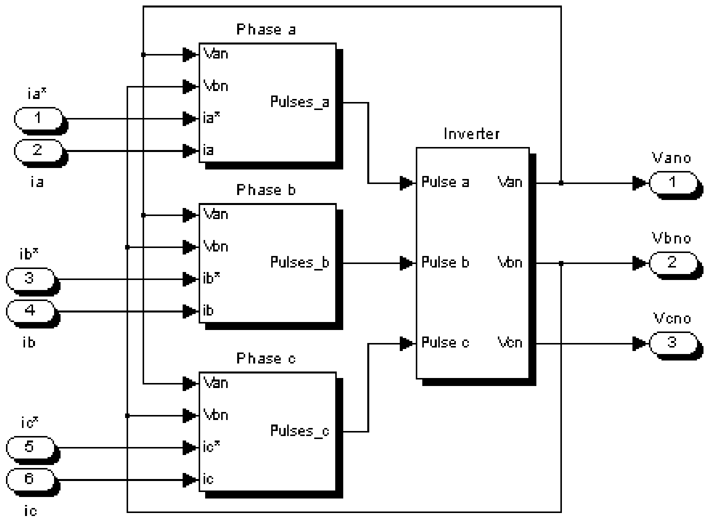

Figure (c.1) Interconnection of the three adaptive hysteresis controllers

To save space (and due to symmetry), modeing of equation (C.1)-(C.2) for phase (a) only will be considered and has been shown in (8).

It should be noted that the modulated equation of adaptive hysteresis controller (inside adaptive hysterresis block of Fig.(8)), given by

$$\begin{aligned}
&\text{if } \Delta I > h \text{ Then } y_h = 1,\\
&\text{if } -h \le \Delta I \le h \text{ and } d\Delta I/dt > 0 \text{ Then } y_h = 1,\\
&\text{if } -h \le \Delta I \le h \text{ and } d\Delta I/dt < 0 \text{ Then } y_h = -1\\
&\text{if } \Delta I < -h \text{ Then } y_h = -1.
\end{aligned} \qquad \text{(C.4)}$$

Is wrritten in s-fuunction file, which is saved as an m-file and contains the protocol in which SIMULIINK can access information from MATLAB

(D)

S-Functin of Adaptive hysteresis-Band Current Controller

```
function [sys,x0,str,ts]= sfunction_hysteresis controller (t,x,u,flag,Ts);

%  This s-function receive three inputs, error, and change of error and the value of the

%  hystersis band, which are passed from the SIMULINK model into the vector u.

% The output  of the s-function is the output of its corresponding s-function block.


if flag= =0,            % Initialization

[sys,x0,str,ts]=mdlInitializeSize(t,x,u,Ts);

% Return the size, initial conditions, and sample times for the s-function

elseif flag= =1          % Derivative : Return the derivatives for the continuous states.

sys=mdlDerivative(t,x,u);

elseif flag= =2        % Update

sys=mdlUpdate(t,x,u); % Handel discrete state update, sample time hits, and major time

                      % step

elseif flag= =3        % Outputs

sys=mdlOutputs(t,x,u) % Return the block outputs.

else

sys=[];

end;

function [sys,x0,str,ts]= mdlInitializeSize(t,x,u,flag,Ts)

sys=[0,0,1,3,0,1,1]; % No continuous states, no discrete states, one output and two inputs, %and
one sampling time.

% initial the initial condtions

x0=[];                                          % str is always an empty matrix
```

```
str=[];                                   % intialize the array of sample times
ts=[Ts 0];                                % end mdlInitializeSizes
function sys=mdlDerivativee(t,x,u);
sys=[]; % end mdlDerivatives
function ys=mdlUpdate(t,x,u)
sys=[];                                   % end mdlUpdate
function sys=mdlOutputs(t,x,u)
dI=u(1);                                  % error
I=u(2);                                   % Cange of error
H=u(3);                                   % Hysteresis Band
if (H/2)
sys=1;
elseif  (I
sys=1;
else
   sys=-1
end                                       %  end mdlOutputs
```

References

[1] David M.E. Ingram and Simon D. Round, "A Novel Digital hysteresis Current Controller for an Active Power Filter," Dep. of Electric and Elecrtonic Eng., University of Canterbury, 199

[2] Simone Buso, Luigi Malesani, and Paolo Mattavelli, "Comparison of Current Control Techniques for Active Filter Applications," IEEE Transactions on Industrial Electronics, Vol. 45, No.5, October 1998.

[3] M. Malinowski, "Sensorless Control Strategies for Three - Phase PWM Rectifiers", Ph.D. Thesis, Warsaw University of Technology, Warsaw, Poland – 2001.

[4] Qunying Yao and D.G. Holmes, "A simple, Novel Method for Variable Hysteresis Band Current Control of a Three Phase Inverter with Constant Switching Frequency," IEEE, Department of Electrical and Computer System Engineering, Monash University, Australia, 1993.

[5] Bimal K. Bose "An Adaptive Hysteresis-Band Current Control Technique of a Voltage-Fed PWM Inverter for Machine Drive System, " IEEE Transaction on Industrial Electronics, Vol.37, No.5, October 1990.

[6] Luigi Malesani, Poalo Tenti "A Novel Hysteresis Control Method for Current-Controlled Voltage-Source PWM Inverters with Constant Modulation Frequency," IEEE Transaction on Industrial Electronics, Vol.26, No.1, January/February 1990.

[7] Bimal K. Bose, "Modern Power Electronics and AC Drive," University of Tennessee, Knoxville, Prentice Hall, 2002.

[8] Chee-Mun Ong, "Dynamic Simulation of Electric Machinery Using Matlab/Simulink", Purdue University, Prentice Hall PTR, 1998.

[9] Dal Y. Ohm, "Dynamic Model of Induction Motors for Vector Control", Drivetech, Inc., Blacksburg, Virginia, 2001.

[10] W. Leonhard ," Control of Electrical Drives," Springer Press, Birlin, 1998.

[11] Amjad J. H., "Fuzzy learning enhanced speed control of indirect field orientation controlled induction machine with adaptive hysteresis band current controller", PHD thesis, University of Technology, Al-Rashid college of Engineering and Science, June, 2005.

[12] Math Works, Inc., "SIMULINK user's Guide," Version 2, Jan 1997.

[13] " Short Tutorial on Matlab," Tomas Co., 2004.